ISSN 1330-3651 (Print), ISSN 1848-6339 (Online) https://doi.org/10.17559/TV-20230803000849
Original scientific paper

Research on Control Strategy of High-Speed Grid-Connected FESS (Flywheel Energy Storage System) Based on Dual-PWM Converter

Wenping BU*, Zhilin DING, Shuling FENG, Xing CAI, Yunfang ZHANG, Xiao YU, Wenhao HUANG

Abstract: FESS (flywheel energy storage system) motor is used in important load fields for instance rail transit; meanwhile the power flow is formed through the connection between FESS (flywheel energy storage system) and power grid system, which can critically improve the power flow fluctuation caused by new energy grid integration regarding wind and photovoltaic generation concerning that the motor speed in FESS is related to its energy storage capacity. Aiming at the limitation of current low motor speed in the FESS, this article puts forward a high-speed grid-connected FESS, and designs a model via the proposed dual-PWM two-stage control form, which is named as double closed-loop control. In this article, the FESS, as well as the power grid system, is analyzed and simulated in three stages: charging, pre-grid connection and grid connection. In this way, the flywheel motor speed and DC bus voltage signal are sampled to design the flywheel motor side with the proposed method. Then the grid-connected double closed-loop control method is designed for the sampling observation points, which realizes the efficient design on the control strategy of proposed high-speed grid-connected FESS and the verification of voltage and current parameters. The simulation experiments show that the operation process of the grid-connected FESS motor obtains its rapid speed response characteristic, which can meet the proposed design requirements during the charging and discharging process.

Keywords: dual-PWM converter; grid-connected control; high-speed FESS; two-stage control

1 INTRODUCTION

The global energy shortage is becoming increasingly serious, and renewable energy has been greatly developed, which has brought about the stability as well as reliability issues regarding the power grid characteristic. The proportion of renewable generation in traditional energy units has increased to constitute a new power system structure [1]. Under the role of the new power system, by connecting the ES (energy storage) unit in the network, the user demand concerning the side of power supply can be adjusted, the supply and demand balance pressure of the load side user can be alleviated, and the system stability can be improved [2]. Countries around the world, such as China, the United States, the United Kingdom, Iran and Nigeria, have conducted research on energy storage technology to improve the stability of power systems [3-9], breaking through the key technology of large-scale energy storage in the power system [10], developed a variety of energy storage structure forms [11], forming an energy storage scheme suitable for different places and environments [12-14]. Flywheel energy storage has attracted amount of attention concerning a competitive ES (energy storage) technology in the current energy 'carbon peak and carbon neutrality' due to its significant advantages of large instantaneous output, long life, low loss and not limited geographical environment [15-19]. Literature [20] described and studied the specific application technology of ES (energy storage) technology concerning the power system from the user demand side, including the system operating voltage quality requirements, the differentiated demand of equipment load level on power quality. The FESS technology is compared from the load level as a demand point, starting from the power demand side. The particularly important load above the first load needs to use the flywheel energy storage and diesel generator set combination system to meet the system demand. Literature [21, 22] compared and analyzed the FESS technology from the aspects of energy storage motor structure characteristics, intermediate power electronic devices, mechanical bearings, motor materials and power quality. By its comparison of reluctance motor, induction motor, and PMSM (permanent magnet synchronous motor), from which can be inferred that although the PMSM is higher in unit cost, its high efficiency can make up for the cost defects to a greater extent, thereby improving the application scope of PMSM as FESS technology. Literature [23] used the current control method to design the FESS applied to the satellite system; at the same time the Z-N algorithm and the current control method were compared and analyzed by using the Bode plot to analyze the system stability, system step response, torque output and voltage and current parameter characteristics. From the perspective of flywheel energy storage multi-parameter control and grid connection, literature [24-26] analyzed the characteristics of each parameter under FESS operation, and the normality and stability of the proposed system is provided with a certain parameter test guarantee combined with its power flow. Literature [27, 28] estimated and analyzed parameters such as response state, voltage, and current fluctuation from the perspective of flywheel energy storage operation fault detection, providing data support for scene parameter estimation under the continuous access of new energy. Concerning the speed of the FESS is proportional to its power capacity, therefore, in order to enhance the FESS power capacity, this paper establishes a high-speed grid-connected FESS based on the flywheel technology. In order to suppress the harmonic injection in the procedure of grid-connected FESS, this paper uses L-type filter to design grid-connected port connector, and uses dual PWM two-stage control mode to control the parameters of grid-connected side and flywheel energy storage motor side in real time, so as to achieve three stages in the process of grid-connecting: charging, pre-grid-connected and grid-connected. Observe the matching degree between flywheel energy storage motor speed, DC voltage stability state and system preset state, and compare and analyze the voltage and current operation state of grid-connected side. By comparing and analyzing the above-mentioned three states with the collected observations, this paper establishes its operation mode and the power grid improvement effect of FESS.

2 FESS STRUCTURE AS WELL AS GRID-CONNECTED DESIGN SYSTEM

2.1 Structural Design of FESS

There are several parts in FESS (Flywheel Energy Storage System), which include the bidirectional DC-AC converter, the PMSM (Permanent Magnet Synchronous Motor) and the flywheel motor, and its structure is shown in Fig. 1. The bidirectional DC-AC converter realizes the connection of the FESS to the large grid through the energy exchange function, optimizing energy management. Actually, during operational procedure, considering the margin between the converter output current and the DC voltage, the operating equation of the FESS under the $i_d - i_q$ plane can be obtained through the output FESS parameters, which can be expressed as follows:

$$\begin{cases} \left(L_d i_d + \psi_f\right)^2 + \left(L_q i_q\right)^2 \le \left(\dfrac{U_{\mathrm{DC}}}{\sqrt{3} p \omega_r}\right)^2 \\ i_d^2 + i_q^2 \le I_{\max}^2 \\ 1.5 p\left[\psi_f i_q + \left(L_d - L_q\right) i_d i_q\right] = T_e \end{cases} \tag{1}$$

In the formula, U_{dc} represents the converter voltage of the DC side, $I_{\max}$ represents the converter output current vector ψ_f maximum value, which also means the permanent magnet flux linkage, L_d represents the stator d-axis inductors, and L_q represents d-axis inductors, and p represents the pole pairs number, i_d represents the stator d-axis current and i_q represents the stator q-axis current, and T_e represents the motor electromagnetic torque. Via depicting the above equation, the charging mode and discharging mode operation strategy diagram of the FESS can be obtained as represented in Fig. 2. Via the current as well as speed loop as the feedback control quantity modulation control during the start-up charging process, the two-stage control method of current and voltage loop is adopted in the process of stable discharge of the system.

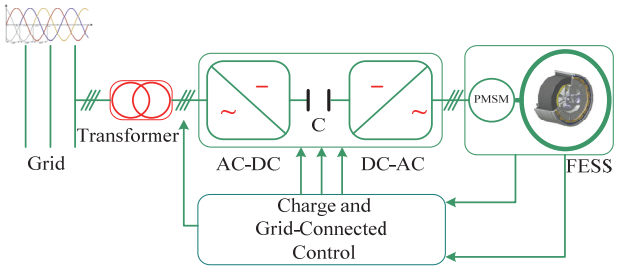

Figure 1 The proposed high-speed grid-connected FESS Structure diagram

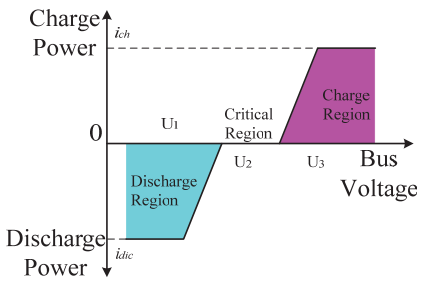

Figure 2 Operation and control strategy of the proposed FESS

2.2 Grid-Connected Design of FESS

In the grid-connected design, the output impedance of the bidirectional energy storage converter can be expressed as $Z_o(s) = 1/Y_o(s)$, its Norton equivalent circuit is shown in Fig. 3, and the grid current transfer function expression can be established according to the superposition principle.

$$\begin{aligned} i_g(s) &= \frac{Z_o(s) G_c(s) i_g(s)}{Z_o(s) + Z_g(s)} - \frac{u_g(s)}{Z_o(s) + Z_g(s)} = \\ &= \left(G_c(s) i_g(s) - \frac{u_g(s)}{Z_o(s)}\right) \frac{1}{1 + \dfrac{Z_g(s)}{Z_o(s)}} \end{aligned} \tag{2}$$

$$H(s) = \frac{1}{1 + \dfrac{Z_g(s)}{Z_o(s)}} \tag{3}$$

The current transformation in the grid-connected process reflects the operating condition of the current, which is the evolution of the small signal model, assuming that when removing the grid-connected inverter, it will be inferred that the grid voltage u_g remains stable; when impedance of the grid is set to zero, then the output impedance of inverter $Z_o(s)$ remains stable, and the fundamental stability of the grid-connected current will be regulated by $H(s)$.

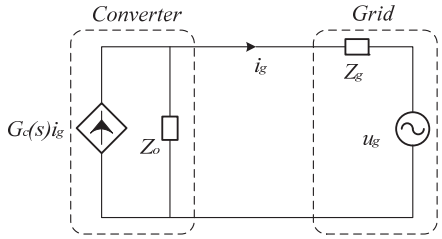

Figure 3 Grid-connected inverter norton equivalent model diagram

During the grid-connected process, the harmonic interference model can be established, as represented in Fig. 4, and there the grid-connected current equation can be written through the transfer function:

$$i_{gh}(s) = -\frac{u_{gh}(s)}{Z_o(s) + Z_g(s)} = -\frac{u_g(s)}{Z_o(s)} \cdot \frac{1}{1 + \dfrac{Z_g(s)}{Z_o(s)}} \tag{4}$$

Through Eq. (4), the harmonics in the grid-connected process can be analyzed, and the grid-connected parameters are designed regarding the harmonic content in order to meet the system requirements.

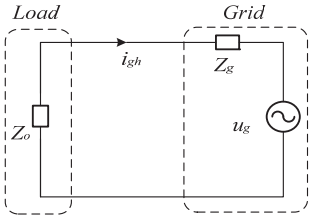

Figure 4 Grid-connected current harmonic injection equivalent model

The FESS access to the power grid, and the closed-loop feedback system is designed regarding the flywheel motor parameters including voltage, speed and current, and the voltage and current vector parameters of the power grid are considered at the same time so that the FESS as well as the grid will be smoothly carried out in the process of grid-connected, forming a closed-loop feedback channel in the charging, pre-grid and grid-connected stages of the FESS.

3 PARAMETER DESIGN AS WELL AS GRID-CONNECTED ANALYSIS OF HIGH-SPEED FESS

3.1 ESS (Energy Storage System) Designing

Generally, the operating state of the FESS can be expressed by its stored energy calculation formula as follows:

$$E = \frac{1}{2} J\omega^2 \tag{5}$$

In the formula, E represents the energy value of FESS, ω represents the motor angular velocity, J represents the motor inertia moment. Via observing Eq. (5), it will be inferred that the energy capacity of FESS is related to its angular velocity ω and moment of inertia J. In the actual design process, if the flywheel design is completed, its energy storage capacity improves in the later stage; its angular velocity growth is an effective method. Indeed, the differential energy ΔE can be regulated or adopted by the FESS and can be expressed as follows.

$$\Delta E = \frac{1}{2} J\omega_{rH}^2 - \frac{1}{2} J\omega_{rL}^2 \tag{6}$$

In the rated speed there is the highest rated speed, denoted as ω_{rH} , the lowest rated speed, denoted as ω; usually the highest rated speed is 2 times the lowest rated speed, ie $\omega_{rH} = 2\omega_{rL}$. At that time $\omega_{rH} = 2\omega_{rL}$, the flywheel reaches FESS capacity maximum value of the design.

$$\Delta E = \frac{1}{2} J\left(2\omega\right) - \frac{1}{2} J\omega = 1.5J\omega \tag{7}$$

The flywheel motor adopts PMSM, through the control strategy analysis and FESS modeling, the current energy parameter of the flywheel rotor as well as PMSM are represented under the dq shaft system.
First, the motor voltage equation is expressed as follows:

$$\begin{cases} u_d = R_s i_d + \dfrac{d\psi_d}{dt} - p\omega_r \psi_q \\ u_q = R_s i_q + \dfrac{d\psi_q}{dt} - p\omega_r \psi_d \end{cases} \tag{8}$$

and the motor magnetic field equation is expressed as follows:

$$\begin{cases} \psi_d = L_d i_d + \psi_f \\ \psi_q = L_q i_q \end{cases} \tag{9}$$

the motor torque equation is expressed as follows:

$$T_e = 1.5p\left[\psi_f i_q + \left(L_d - L_q\right) i_d i_q\right] \tag{10}$$

Equations of motion:

$$T_e = T_l + J\frac{d\omega_r}{dt} + B\omega_r \tag{11}$$

In the formula, u_d represents stator d-axis voltage and u_q represents stator q-axis voltage, i_d as well as i_q represent the stator d-axis current and q-axis current, R_s represents the stator resistance, ψ_d represents the motor d-axis flux linkage and ψ_d represents the motor q-axis flux linkage, respectively. ω_r represents the motor mechanical angular velocity, L_d as well as L_q represent the stator d-axis inductors and stator q-axis inductors, respectively. Ψ_f means permanent magnet fluxes, p represents the magnetic pole pairs number, and T_e represents the motor electromagnetic torque, T_l represents the motor load torque, J represents the inertia moment, and B represents the friction coefficient.

3.2 Design of High-Speed Fess Concerning Grid-Connected Control System

At first, the proposed high-speed FESS needs to connect to the power grid during operation, and the energy conversion and connection is carried out through the converter in the middle, and the excess electrical energy is converted into the motor mechanical energy via the high-speed FESS when the energy on the grid side is surplus, which results in the flywheel energy being transmitted into electric energy via the grid. Then, in the process of grid connection, it is necessary to design the connection port filter to meet the indicators of the power grid, as shown in Fig. 3 where the grid-connected FESS structure is based on the Norton equivalent circuit, and the output is formed by calculating its transfer function and connecting it in series with the input parameters, which provides a basement for the indicators parameter designing. If the harmonic injection on the energy storage side of the grid is considered, the proposed equivalent model concerning the harmonic content circuit as shown in Fig. 4 can be obtained. The design of the filter needs to consider the energy relationship between the FESS as well as the grid, which includes charging, pre-grid-connected, and grid-connected mode.

3.2.1 Charging

In the charging stage, the connection between the high-speed FESS and the power grid is operated under the form of uncontrolled rectification, and the flywheel motor forms loop control through the form of motor speed and current monitoring, accelerates the FESS to the specified speed, and uses the FESS structure to form energy storage,

as shown in Fig. 2 charging area segment.

3.2.2 Pre-Grid-Connected

After the charging mode, the FESS yields the set speed, the control form of the converter on the grid side remains unchanged, and then the FESS motor is switched from the speed current loop to the current and voltage loop control at the loop control end, and the grid connection conditions are provided for the pre-grid-connected stage of energy conversion by monitoring the system voltage. When the FESS motor injects energy into the grid side, the FESS motor voltage is larger than the voltage on the grid side to form grid-connected operating conditions, as shown in Fig. 2.

3.2.3 Grid Connection

After the FESS access to the power grid, converter in the grid-side adopts the grid-side bus to detect voltage and current variables to form a loop, and the power control mode of the current and voltage on the motor side is carried out to complete the power conversion process between the DC bus and the power grid. In this process, the converter adopts a dual-PWM control mode to facilitate the energy flow of grid-connected energy from the mechanical energy of FESS to the electrical energy of the grid, forming an expected power flow operation, as shown in Fig. 2 discharge area segment.

4 OPERATION RESULTS AND ANALYSIS OF GRID-CONNECTED MODE OF HIGH-SPEED FESS

This section, in order to verify the rationality of the control method of the improved speed flywheel energy storage grid-connected system, a model with high-speed grid-connected FESS was built, and the simulation experimental research of high-speed FESS from charging to grid connection was completed, and the high-speed grid-connected FESS parameters are represented in Tab. 1, and the simulated grid-connected experimental model is pictured in Fig. 5, respectively. Then Tab. 1 regulates the design parameters of the high-speed FESS, which are tabulated as follows.

Table 1 Proposed high-speed grid-connected FESS parameters

Parameter	Numeric Value	Parameter	Numeric Value
The flywheel motor rated speed n	9950 rpm	Filter inductor L	8 mH
Flywheel motor rated capacity S	13000VA	DC side voltage U_{DC}	1000 V
The flywheel motor pole pair p	2	Grid voltage U_g	400 VAC
Flywheel motor rated current I	21A	Grid frequency f	50 Hz
Flywheel motor moment of inertia J	0.05 $\mathrm{kg \cdot m^2}$	Filter capacitor C	3 mF

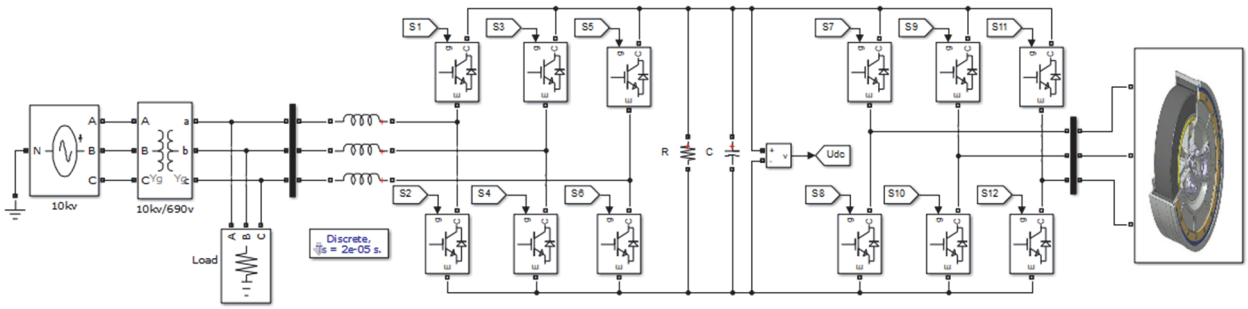

Figure 5 Model diagram of high-speed grid-connected FESS

The circuit structure of simulation experiment is shown in Fig. 5, which includes power grid module, filter module, converter module and FESS module. From the parameter data represented in Tab. 1, the dual-PWM converter switching frequency is set at 10 kHz. By setting the simulation time length of 9s, the charging completion time of the proposed high-speed FESS is 6 s, and the pre-grid-connected time is 1 s. Starting from 7 s, three state modes of charging, pre-grid-connected and grid-connection of high-speed FESS are established. Owing to the limited voltage fluctuation range in the steady-state between charging and discharging process, this paper can effectively reflect the running state of the proposed high-speed grid-connected FESS by taking the grid-connected current as the monitoring variable.

Fig. 6 represents the waveform diagram of DC voltage and flywheel speed signal of the FESS based on the control mode. From the picture, it can be seen from observation that this paper uses mode bit 1, 2 and 3 to set the three states of charging, pre-grid-connected and grid-connected of the FESS switching to the status between 5 s and 6 s. During the charging process of the FESS motor, the DC voltage of the uncontrolled rectifier part of the power grid represents its stability in the range of 925 VDC, and the speed of the flywheel motor continues to increase from zero.

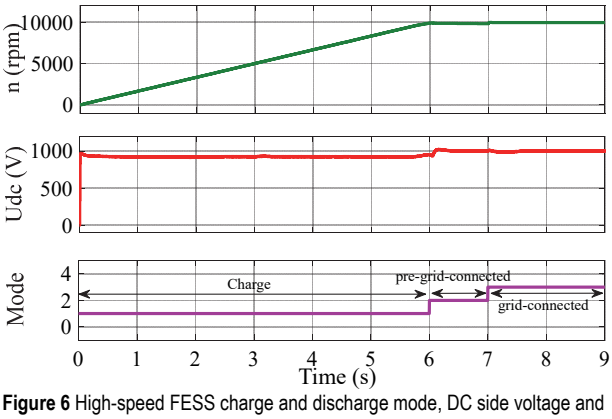

Figure 6 High-speed FESS charge and discharge mode, DC side voltage and motor speed sampling signal waveform

Currently, the motor speed and voltage ring action, the motor is finally stable in the rated speed of 9950 rpm range. In the pre-grid-connected and grid-connected links, the DC voltage as well as the flywheel motor speed remain unchanged. The system transits from the current and speed loop to the voltage and current loop, as shown in Fig. 7.

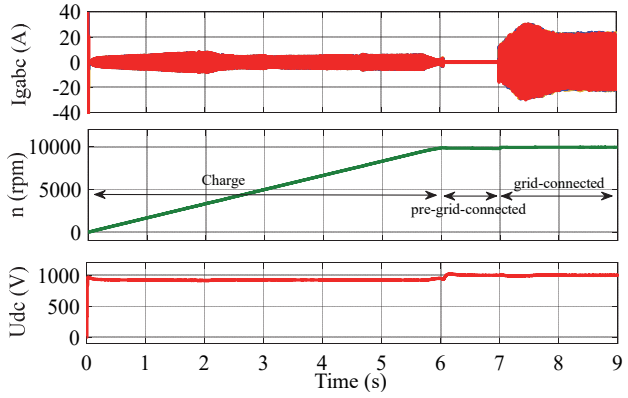

Figure 7 DC-side voltage, motor speed and grid-connected side current sampling signal waveform in high-speed FESS charge-discharge mode

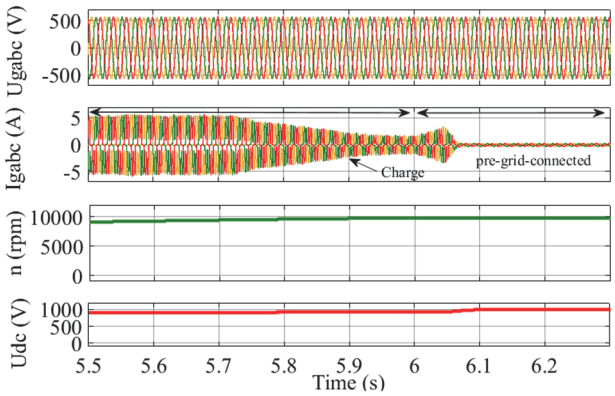

Figure 8 High-speed FESS charging-state sampling signal waveform in pre-grid-connected mode

Here, it is depicted from Fig. 7 that the motor charging current in the charging process remains relatively stable, which is used to absorb the power grid energy; at this time, the charging current of the flywheel motor is stable at 3.85 A, the pre-grid-connected transition to the grid-connected process. The flywheel motor maintains the stable voltage during the external energy conversion process, and the current gradually transitions to a stable state of 19.9 A, realizing the discharge regarding the grid, and the grid-connected FESS process reaches the grid-connected stable state after 1s, and the response speed is fast. By observing the DC side voltage, flywheel motor speed, grid-connected side current and voltage signal, the multi-parameter monitoring of the FESS in charging, pre-grid-connected and grid-connected status is realized, which can effectively grasp and realize the operation of high-speed grid-connected FESS. As represented in Fig. 8, the high-speed grid-connected FESS adopts signal waveform between the charging process and the pre-grid-connected process, and the sampling time point is 5.5 - 6.3 s. The system is charged to the end at 6 s, and 6 s - 7 s is the pre-grid-connected process to prepare for grid-connection. The figure shows that the DC voltage and the grid voltage remain in stable operation. The speed of the flywheel motor also changes from the acceleration state to the rated speed state, and the current on the grid-connected side changes from the charging state to the pre-grid-connected state. In this paper, the synchronous state of voltage, frequency and phase detection is realized. The *RMS* voltage of the AC side is 400 V, the current of the energy storage motor is non-sine wave containing harmonics, the peak current of the charging process is 5 A, the peak current of the pre-grid-connected procedure is 0.37 A, and the peak current value during the grid-connected stage is 28.3 A.

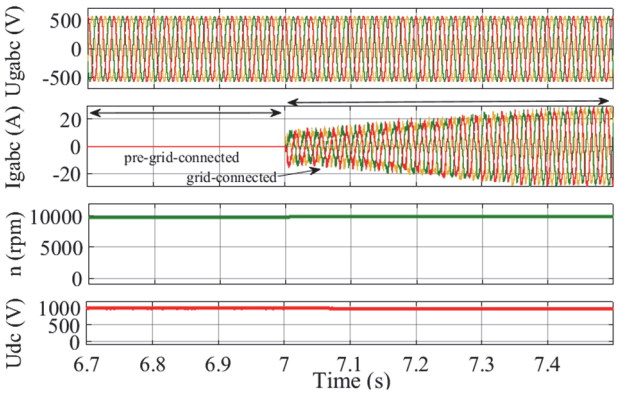

Figure 9 Waveform of high-speed FESS pre-grid-connected state sampling signal in grid-connected mode

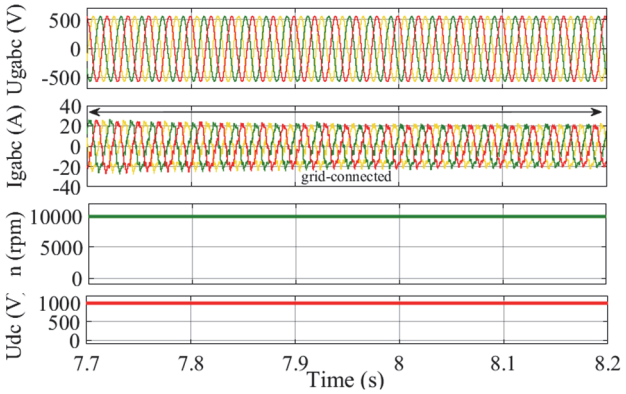

Figure 10 Waveform of state-sampled signal in high-speed FESS grid-connected mode

As represented in Fig. 9 the proposed high-speed grid-connected FESS changes from pre-grid-connected to grid-connected transition state, which is inferring that the DC voltage, motor speed and grid-connected side voltage signal remain stable, the FESS realizes the discharge procedure of the main power grid through the voltage as well as the current loop, and the system is converted from pre-grid-connected to grid-connected at 7 s, then the ESS (energy storage system) is discharged to the main grid to realize energy feedback, and the grid-connected side current gradually increases until the rated output power of the ESS reaches variable at 19.9 A. As is depicted in Fig. 10 that the signal waveform is in the high-speed grid-connected FESS mode, inferring that the waveform data of each adopted signal is in a stable state, the FESS releases energy to the main power grid stably, and the electrical energy is converted from mechanical energy to the main power grid; at this time the sampling time is depicted between 7.7 s - 8.2 s, representing voltage of the DC side by 1000 V, the FESS motor speed by 9950 rpm,

the main grid current by 19.9 A, and the main grid voltage by 400 V.

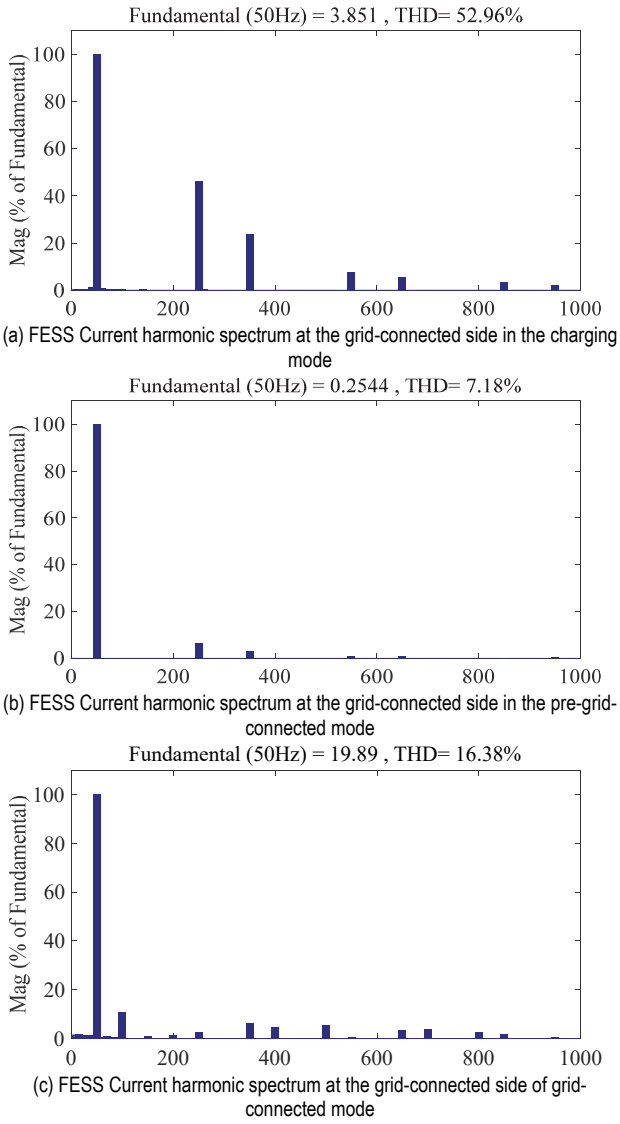

(a) FESS Current harmonic spectrum at the grid-connected side in the charging mode

(b) FESS Current harmonic spectrum at the grid-connected side in the pre-grid-connected mode

(c) FESS Current harmonic spectrum at the grid-connected side of grid-connected mode

Figure 11 Current harmonic spectrum at each mode of the grid-connected FESS

Actually, in the grid-connected procedure, its voltage maintains low harmonic interference, but the current is harmonic due to the power device, and the relationship between the FESS operation as well as the current harmonics of the power grid can be all observed through harmonic analysis of the current. As shown in Fig. 11, the current harmonic analysis diagram of the grid-connected FESS in the charging, pre-grid-connected and grid-connected stages shows that the grid-connected FESS procedure has an improving effect on the harmonics of the system, and the grid-connected FESS promotes the improvement of the power quality on the grid side. Taking 50 Hz as the fundamental frequency, which infers that the grid-connected can weaken the 5th and 7th harmonic content on the grid operating side, while in the pre-grid stage of Fig. 11b, depicting that the comprehensive harmonic content regarding the grid current gets the lowest value by only 7.18%, and the harmonic content of Fig. 11c after grid connection is 16.38%, compared with 52.96% in the charging stage of Fig. 11a, the harmonic content of the grid side is effectively improved.

5 CONCLUSION

In order to enhance the flywheel energy storage capacity and achieve the grid integration of the FESS and the power grid system, this article designs the structure of high-speed grid-connected FESS based on dual-PWM converter and its two-stage control method compared to the traditional low-speed FESS. Successively this article establishes the operation structure of the grid-connected FESS, the working principal mode of the grid-connected FESS and the model. The proposed control method concerning double closed-loop which includes the speed and voltage in the charging stage and the current and voltage in the pre-charging and grid-connected stage are constructed, and then the system operating parameters are observed by combining the monitoring variables such as DC side bus voltage and flywheel motor speed. The results infer that FESS can achieve stable control of the voltage on the grid-connected side during the charging as well as discharging procedure, and the speed control of the charging procedure of the FESS can be realized through the speed loop as well as the current variable loop on the grid-connected side, reaching the motor rated speed by 9950 rpm and the current by 19.9 A to realize the external energy supply function, and the harmonic current analysis of the FESS shows that the harmonic content of the current with the FESS access to the grid is 16.38%, which has a great improvement effect on the harmonic content of the power grid in the charging stage of 52.96%.

Acknowledgments

This research was funded by Jiangxi Province College Student Innovation and Entrepreneurship Training Program Project (s202213421006, s202213421003), Nanchang Institute of Science and Technology Campus Level Key Project (NGJG-2022-08), Nanchang Institute of Science and Technology Teaching Team Cultivation Project (JXTD-PY-15).

6 REFERENCES

[1] Suhang, Y., Wenyong, G., & Yuping, T., et al. (2021). A review of the structures and control strategies for flywheel bearings. *Energy Storage Science and Technology*, *10*(05), 1631-1642.

[2] Jianli, Z., Zhuofan, T., & Guilin, W., et al. (2022). Operation characteristics of user-side resources with energy storage function. *Integrated Intelligent Energy*, *44*(02), 8-14.

[3] Soomro, A., Pullen, K. R., & Amiryar, M. E. (2021). Hybrid PV System with High Speed Flywheel Energy Storage for Remote Residential Loads. *Clean Technologies*, *3*(2), 351-376. https://doi.org/10.3390/cleantechnol3020020

[4] Tziovani, L., Hadjidemetriou, L., & Charalampous, C., et al. (2021). Energy Management and Control of a Flywheel Storage System for Peak Shaving Applications. *IEEE Transactions on Smart Grid*, *12*(5), 4195-4207. https://doi.org/10.1109/TSG.2021.3084814

[5] Mahdavi, M. S., Gharehpetian, G. B., & Moghaddam, H. A. (2020). Enhanced Frequency Control Method for Microgrid-Connected Flywheel Energy Storage System. *IEEE Systems Journal*, *15*(3), 4503-4513. https://doi.org/10.1109/JSYST.2020.3010029

[6] Shena, L., Cheng, Q., & Cheng, Y., et al. (2020). Hierarchical control of DC micro-grid for photovoltaic EV

charging station based on flywheel and battery energy storage system. *Electric Power Systems Research*, *179*(2020), 106079. https://doi.org/10.1016/j.epsr.2019.106079

[7] Ayodele, T. R., Ogunjuyigbe, A. S. O., & Oyelowo, N. O. (2020). Hybridisation of battery-flywheel energy storage system to improve ageing oflead-acid batteries in PV-powered applications. *International Journal of Sustainable Engineering*, *13*(5), 337-359. https://doi.org/10.1080/19397038.2020.1725177

[8] Mir, A. S. & Senroy, N. (2019). Intelligently Controlled Flywheel Storage for Enhanced Dynamic Performance. *IEEE Transactions on Sustainable Energy*, *10*(4), 2163-2173. https://doi.org/10.1109/TSTE.2018.2881317

[9] Mansour, M., Mansouri, M. N., & Bendoukha, S., et al. (2019). A grid-connected variable-speed wind generator driving a fuzzy-controlled PMSG and associated to a flywheel energy storage system. *Electric Power Systems Research*, *180*(2019), 106137. https://doi.org/10.1016/j.epsr.2019.106137

[10] Xing, Z., Peng, R., & Liuli, Z., et al. (2021). Performance test of flywheel energy storage device. *Energy Storage Science and Technology*, *10*(05), 1674-1678.

[11] Wenjun, L., Dongqiang, J., & Haomin, Z., et al. (2021). Development and Engineering Application Status of Flywheel Energy Storage System. *Smart and Special Electrical Machines*, *49*(12), 52-58.

[12] Yong, Z., Xiangyu, C., & Lin, J., et al. (2022). Design and experimental research on flywheel energy storage system of beam pumping unit. *Energy Storage Science and Technology*, *11*(02), 593-599.

[13] Ying, X. C., Zhi, G. Z., & Hong, W. X., et al. (2022). Control Strategy of Flywheel and Battery Hybrid Energy Storage in Wind Power System. *Journal of Shenyang Institute of Engineering (Natural Science)*, *18*(01), 12-19.

[14] Jin, L., Gang, Z., & Zhigang, L., et al. (2021). Control Strategy of Flywheel Energy Storage Array for Urban Rail Transit. *Transactions of China Electrotechnical Society*, *36*(23), 4885-4895. https://doi.org/10.1007/978-981-16-9905-4_5

[15] Yulong, C., Xin, W., & Wei, T., et al. (2022). Power coordinated control strategy of flywheel energy storage array for wind power smoothing. *Energy Storage Science and Technology*, *11*(2), 600-608.

[16] Mei, J., Tingxin, Y., & Liguo, Z., et al. (2021). Finite Element Analysis and Experimental Analysis for 200 kW /180 MJ Flywheel Energy Storage System. *ACTA Metrologica Sinica*, *42*(7), 885-891.

[17] Wang, Y., Wang, C., & Xue, H.(2021). A novel capacity configuration method of flywheel energy storage system in electric vehicles fast charging station. *Electric Power Systems Research*, *195*(2021), 107185. https://doi.org/10.1016/j.epsr.2021.107185

[18] Hutchinson, A. & Gladwin, D. T. (2020). Optimisation of a wind power site through utilisation of flywheel energy storage technology. *Energy Reports*, *6*(S5), 259-265. https://doi.org/10.1016/j.egyr.2020.03.032

[19] Awadallah, M. A. &Venkatesh, B. (2015). Energy Storage in Flywheels: An Overview. *Canadian Journal of Electrical and Computer Engineering*, *38*(2), 183-193. https://doi.org/10.1109/CJECE.2015.2420995

[20] Yanyan, Z., Weiqiong, S., & Cheng, Z., et al. (2018). Application of flywheel energy storage equipment in vital places. *Energy Storage Science and Technology*, *7*(5), 847-852.

[21] Amiryar, M. E. & Pullen, K. R. (2017). A Review of Flywheel Energy Storage System Technologies and Their Applications. *Applied Sciences*, *7*(2017), 286. https://doi.org/10.3390/app7030286

[22] G, S. M. M., Faraji, F., & Majazi, A., et al. (2017). A comprehensive review of Flywheel Energy Storage System technology. *Renewable and Sustainable Energy Reviews*, *67* (2017), 477-490. https://doi.org/10.1016/j.rser.2016.09.060

[23] Çelikel, R. & Özdemir, M. A. (2019). Method for Current Control of the Flywheel Energy Storage System Used in Satellites. *Tehnicki Vjesnik-Technical Gazette*, *26*(3), 631-638. https://doi.org/10.17559/TV-20160328090219

[24] Jing, L., Yu, Y., & Xue, X. (2020). A Research on the Control System of High-Speed Homopolar Motor with Solid Rotor Based on Flywheel Energy Storage. *Complexity*, *2020*, 6537563. https://doi.org/10.1155/2020/6537563

[25] Ahamad, N. B. B., Su, C., & Zhaoxia, X., et al. (2019). Energy Harvesting from Harbor Cranes with Flywheel Energy Storage Systems. *IEEE Transactions on Industry Applications*, *55*(4), 3354-3364. https://doi.org/10.1109/TIA.2019.2910495

[26] Dragoni, E. (2017). Mechanical design of flywheels for energy storage: A review with state-of-the-art developments. *Journal of Materials*, *233*(5). https://doi.org/10.1177/1464420717729415

[27] Li, X., Anvari, B., & Palazzolo, A., et al. (2017). A Utility Scale Flywheel Energy Storage System with a Shaft-less, Hub-less, High Strength Steel Rotor. *IEEE Transactions on Industrial Electronics*, *65*(8), 6667-6675. https://doi.org/10.1109/TIE.2017.2772205

[28] Ahsan, H. & Muft, M. (2019). Dynamic performance improvement of a hybrid multimachine system using a flywheel energy storage system. *Wind Engineering*, *44*(3), 239-252. https://doi.org/10.1177/0309524X19849853

Contact information:

Wenping BU
(Corresponding author)
School of Information and Artificial Intelligence,
Nanchang Institute of Science & Technology,
Jiangxi, Nanchang, 330108, China
E-mail: 18770001680@163.com

Zhilin DING
School of Information and Artificial Intelligence,
Nanchang Institute of Science & Technology,
Jiangxi, Nanchang, 330108, China

Shuling FENG
School of Information and Artificial Intelligence,
Nanchang Institute of Science & Technology,
Jiangxi, Nanchang, 330108, China

Xing CAI
School of Information and Artificial Intelligence,
Nanchang Institute of Science & Technology,
Jiangxi, Nanchang, 330108, China

Yunfang ZHANG
School of Information and Artificial Intelligence,
Nanchang Institute of Science & Technology,
Jiangxi, Nanchang, 330108, China

Xiao YU
School of Information and Artificial Intelligence,
Nanchang Institute of Science & Technology,
Jiangxi, Nanchang, 330108, China

Wenhao HUANG
School of Information and Artificial Intelligence,
Nanchang Institute of Science & Technology,
Jiangxi, Nanchang, 330108, China